JOURNAL OF GUIDANCE, CONTROL, AND DYNAMICS
Vol. 30, No. 5, September–October 2007

Fault Detection in Open-Loop Controlled Structures

Shanshan S. McNeill* and David C. Zimmerman†
University of Houston, Houston, Texas 77204

DOI: 10.2514/1.27352

In the past decades, various algorithms have been proposed to detect failed structural members, sensors, and actuators. Most of these works make the assumption that the fault has already been isolated to either the sensors, actuators, or the structure itself. This work provides a novel technique for system-failure detection and classification using the eigensystem realization algorithm and outlier analysis. The technique is based on the comparison of the state-space-form realizations between the current system and the healthy system. Three different failure types of a dynamic system (sensor failure, actuator failure, and structural failure) are studied and compared to determine the unique statistical characteristics of each type of failure mode. Six coefficients representing these patterns are extracted from the realizations of the current system and compared with the generalized benchmarks of the healthy system so that system failure can be diagnosed. An expert system is also developed to automate the diagnosis process. Simulations and experiments successfully validate this work.

I. Introduction

FOR the improvement of reliability, safety, and operational efficiency, failure detection and isolation (FDI) has raised the interest of many researchers. This especially holds true in the fields of aerospace, civil, and mechanical engineering. In the last three decades, improvements in experimental vibration measurement technology coupled with rapid advancements in computing capability have encouraged the development of many new vibration-based techniques for FDI. In these methods, the failure is usually detected by monitoring features of the system. Abnormal changes of the features in the experimental measurements indicate the existence of system failures. These techniques enable remote and online identification of failure on a global basis. Several survey papers include [1–6] and references therein.

The landmark paper of Gertler [7] stated that complete damage detection (DD) consists of detection, isolation, and identification. He proposed two DD categories: model-free and model-based methods. Model-free DD approaches consist of limit checking, special sensors, multiple sensors, frequency analysis, and expert systems [7]. Model-based DD methods consist of parameter estimation, state estimation, and parity equations [8]. For parameter (state) estimation solutions, the change in model parameters (states) is used to generate residuals. For parity equation solutions, an analytical model can be used to estimate a sensor output based on other sensor information. The estimated sensor output can be compared with the actual sensor output to generate a residual. These residuals are then processed to diagnose faults [8]. The residuals generated are a result of combined faults, noise, and modeling errors. DD sensitivity and robustness properties can be quantified by these residuals in which the ability of the algorithm to isolate a fault is strongly related to the modeling errors associated with the residuals.

Most structure-based DD techniques monitor the changes in the damped natural frequencies and mode shapes. Doebling et al. [9,10] and Sohn et al. [11] provided some of the most comprehensive reviews of the technical literature concerning the detection, location, and characterization of structural damage via techniques that examine changes in measured structural vibration response. Other modal-based DD techniques include subspace identification and updating [12,13], evolutionary algorithms [14], minimum rank perturbation theory [15], Ritz vector analysis [16], neural networks [17,18], and Lyapunov exponents [19].

The identification of modal parameters from measured data can be done in a wide variety of ways through many time- and frequency-domain algorithms. Some common modal parameter identification algorithms include the Ibrahim time-domain (ITD) technique [20,21], polyreference algorithm [22], eigensystem realization algorithm (ERA) [23,24], and the observer/Kalman filter identification algorithm (OKID) [25,26]. Among them, a common method for identification of modal parameters is the ERA. Dyke et al. [27] used cross-correlation functions in conjunction with the ERA for identification of the modal parameters, which are used to identify frequency and damping parameters. Caicedo et al. [28] introduced structural health monitoring (SHM) methods based on changes in the component transfer functions of the structure and used the ERA to identify the natural frequencies of each component transfer function. Lus and Betti [29] proposed a damage-identification method based on the ERA with a data correlation and observer/Kalman identification algorithm. Bernal and Gunes [30] also used the ERA with observer/Kalman identification for identifying modal characteristics when the input is known and used a subspace identification algorithm when the input cannot be measured. Zimmerman and Lyde [31] used the ERA to perform FDI for sensor networks.

This paper provides a novel system-failure-detection technique using the ERA and outlier analysis that not only detects the failure but classifies it as either a sensor, actuator, or structural failure. The ERA is used to determine the state-space realization of the system. The state of the system is compared with that of the healthy system and features that indicate damage are extracted. Outlier analysis is used with the extracted features to classify the failure as either a failed sensor, actuator, or structure.

II. Theoretical Background

Because of its ability to handle multi-input/multi-output systems, especially those that are lightly damped, the ERA has become a recognized and successful method for analyzing data in a number of engineering applications since its appearance in 1985. Based on system realization and the singular value decomposition (SVD), the ERA constructs a discrete state-space model of minimal order that fits measured impulse response functions (IRFs) handling closely spaced frequencies to a high degree of accuracy [32]. The first step in the application of the ERA is to obtain impulse response data from either an impulse modal test or the measured frequency response function using the inverse Fourier transform. The ERA then

Received 11 September 2006; accepted for publication 18 May 2007.

*Graduate Student, Mechanical Engineering Department, 4800 Calhoun Road.

†Professor, Mechanical Engineering Department, 4800 Calhoun Road.

determines a minimal order state-space model that best matches the observed input–output characteristics of the structure.

When performing realizations of the same structure using even slightly different data sets (or even different time blocks of the same test), the ERA will perform the realization in different state-space coordinates, making the comparisons of two state-space models meaningless. However, if $[A_1, B_1, C_1]$ and $[A_2, B_2, C_2]$ are two realizations of the same system (both of order n), they can be transformed to the same coordinate system by

$$A_2 = T^{-1}A_1T, \qquad B_2 = T^{-1}B_1, \qquad C_2 = C_1T \tag{1}$$

where $T = Q_1Q_2^{-1}$ or $T = P_1^{-1}P_2$ [33]. Matrices P_1, P_2, Q_1, and Q_2 are the observability and controllability matrices of the two realizations, which are defined as

$$P_i = \begin{bmatrix} C_i \\ C_iA_i \\ \vdots \\ C_iA_i^{n-1} \end{bmatrix}, \qquad Q_i = [\,B_i \quad A_iB_i \quad \cdots \quad A_i^{n-1}B_i\,] \tag{2}$$

$(i = 1, 2)$

By this unique similarity transformation, all of the minimal realizations of a system can be transformed to the same state-space coordinates; this then allows for a meaningful comparison of two state-space models.

Outlier analysis has long been a concern of statisticians, and in recent years, it has begun to be used in SHM [34,35]. Simply speaking, an outlier is defined as an observation (or subset of observations) that appears to be inconsistent with the remainder of the data [36] and is therefore believed to be generated by an alternative mechanism. The discordance of the candidate outlier is a measure that may be compared against some objective criterion. This measure allows the outlier to be judged to be statistically likely or unlikely to have come from an assumed generating model that is simply the normal condition feature of the system. In this paper, the Mahalanobis distance of the system realizations is used as a damage-sensitive feature for outlier analysis. The Mahalanobis distance of the parameters of the current system is compared with that of the baseline healthy system. Damage can then be identified by the existence of outliers and classified by the unique patterns of the outliers.

The Mahalanobis distance is calculated for different realizations of the healthy system and current system, which is a set consisting of n observations in p variables. For a p-dimensional multivariate sample X_ς $(\varsigma = 1, 2, \ldots, n)$, the corresponding Mahalanobis distance is given as

$$D_\varsigma = (X_\varsigma - \bar{X})^T[S]^{-1}(X_\varsigma - \bar{X}) \tag{3}$$

where $\bar{X}$ is the mean vector of the entries X_ς in the data set and S is the sample covariance matrix. Mahalanobis discordance D_ς is also sometimes referred to as the Mahalanobis least-squares distance (MLSD). The Mahalanobis discordance of the potential outlier is checked against a threshold value to determine its status.

III. Algorithm and Numerical Studies

Based on the ERA and outlier analysis, the algorithm for failure detection and classification is developed and summarized by the following steps:

1) Obtain a group of realizations of the healthy system from the input and output time series. What differs between each group is either that

a) They were obtained from independent tests of the baseline structure.

b) In the case of only one test, the test data have been corrupted by numerical noise to simulate the anticipated variability in the test setup.

2) Each row of the state matrix A and output influence matrix C and each column of the input influence matrix B is considered as an observation. Using Eq. (3), the discordance data pool of the system parameters (A, B, C, and damped natural frequencies) of the healthy system is computed. The MLSDs of the realizations of the healthy system will be used as the normal condition features of the system. For the system in a normal working condition, what differs between each realization is the experimental noise that influenced each realization.

3) Obtain the realizations of the current system. Using the same average and covariance matrices as used in step 2, the MLSDs of the current realization are computed, which represent the change of the system parameters in the current system and outliers that are expected in the MLSDs of a damaged system.

4) Because of dynamics properties, different system failures will give different statistical patterns in the detected outliers. A diagnosis process extracts the patterns of the outliers and compares them with the benchmarks of some decision coefficients to identify and classify the failure.

A spring-mass-damper system, shown in Fig. 1, is chosen for the initial characterization of the algorithm. The analytical model is given by the mass M and stiffness K matrices:

$$M = 10^1\begin{bmatrix} 10 & 0 & 0 & 0 & 0 \\ 0 & 3 & 0 & 0 & 0 \\ 0 & 0 & 5 & 0 & 0 \\ 0 & 0 & 0 & 7 & 0 \\ 0 & 0 & 0 & 0 & 9 \end{bmatrix}, \qquad K = 10^4\begin{bmatrix} 13 & -5 & 0 & 0 & 0 \\ -5 & 6 & -1 & 0 & 0 \\ 0 & -1 & 10 & -9 & 0 \\ 0 & 0 & -9 & 14 & -5 \\ 0 & 0 & 0 & -5 & 12 \end{bmatrix} \tag{4}$$

Modal damping was defined with modes 1 through 5 having 3, 2.5, 2, 1.5, and 1% of critical damping.

First, a multi-input case is studied for the given system. Three actuators are assumed to be located at masses 1, 3, and 5, respectively. It is assumed that the displacement of each mass is measured. When there is no damage existing in a current system, all of the system parameters of the current system are expected to be the same as those of the healthy system. No significant outliers in the system parameters should be observed; this can be verified by Fig. 2, which shows the discordance patterns of a system without damage. The first 100 trials represent the healthy system and trials 101–200 represent the current system, which is compared with the healthy system for a possible failure. There are no significant differences between trials 1–100 and 101–200. Note that both the output of the healthy system and the current system time histories are corrupted by 5% random noise.

Damage in structures is typically either a reduction in stiffness or mass. For sensor or actuator failure, it could be because of the total malfunction of the sensor or actuator (called *dead*) leaving only noise or just a gain change (called *damaged*). Different system failures (structural damage, sensor dead/damage, and actuator dead/damage) are all simulated using the system shown in Fig. 1.

Figure 3 show the discordance patterns of the A, B, and C matrices and the natural frequencies when the gain of sensor 1 is reduced by 80%, which represents a sensor-damage case. Notice in trials 101–200 that there is very little change in the discordances associated with matrices A and B and the identified natural frequencies, whereas there is a significant change in discordances in the C matrix. In addition, note that the large discordance changes in the C matrix are associated with row 1, which correctly identifies which sensor has been damaged; this proper localization can be explained. With a sensor gain failure, what effectively has occurred is a change in the physical eigenvector component at the failed sensor degree of freedom. The identified natural frequencies and damping ratios

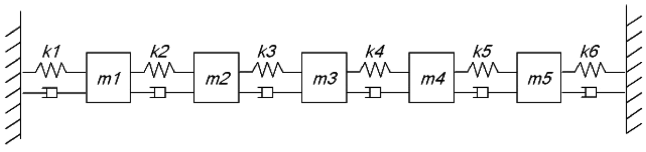

Fig. 1 Analytical spring-mass-damper system.

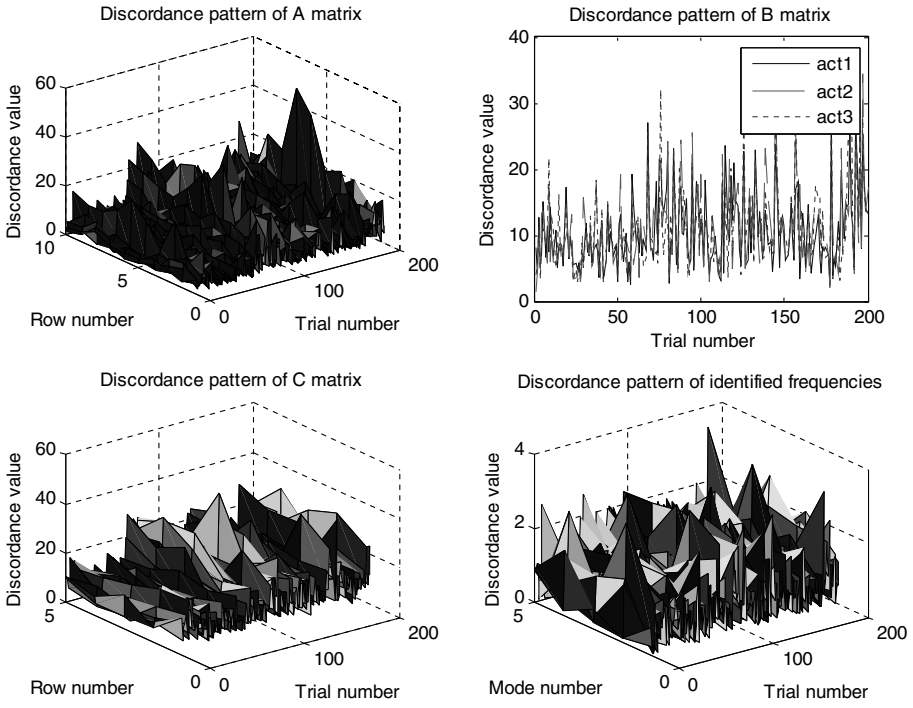

Fig. 2 Discordance pattern of a healthy system.

remain effectively the same as in the healthy system (except for slight changes due to different noise). The output influence matrix C maps state-space eigenvectors into physical eigenvectors and thus a change in the physical eigenvector naturally is accounted for in this matrix.

Figure 4 shows that the discordances associated when the values of $m4$ and $k2$ are reduced by 50% (structural damage). In this case, all three state-space matrices show large discordance values after damage, as do the identified natural frequencies, because the underlying eigenstructure is now different from the healthy system. Figure 5 shows a comparison of the discordance patterns of the healthy system and the current system when the actual input of the second actuator, which is attached to $m3$, is replaced by a zero command. There are no outliers observed in the identified natural frequencies of the damaged system (which is different from the structural damage case), because the remaining actuators are fundamentally exciting the same healthy structure.

Simulations reveal that for different types of failure, the studied parameters show uniquely different discordance patterns. For example, for a dead or damaged sensor, the C matrices show large outliers in the row corresponding to the damaged sensor, whereas the other parameters do not show observable outliers. For structural damage, not only do the A, B, and C matrices show a large discordance change, but so do the identified frequencies. For a dead

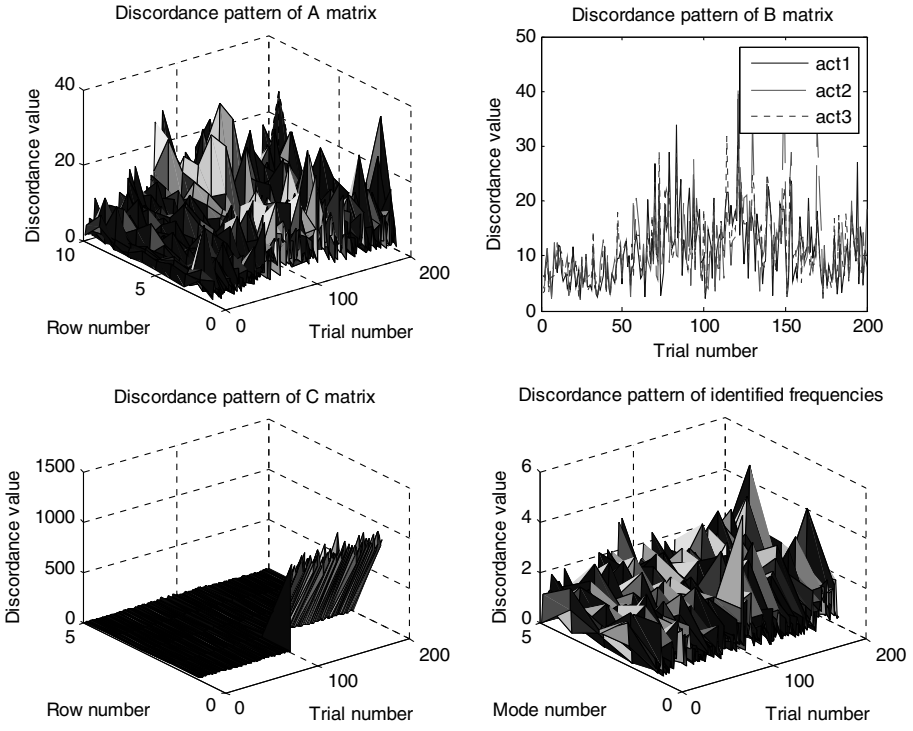

Fig. 3 Discordance pattern of a sensor-damage system.

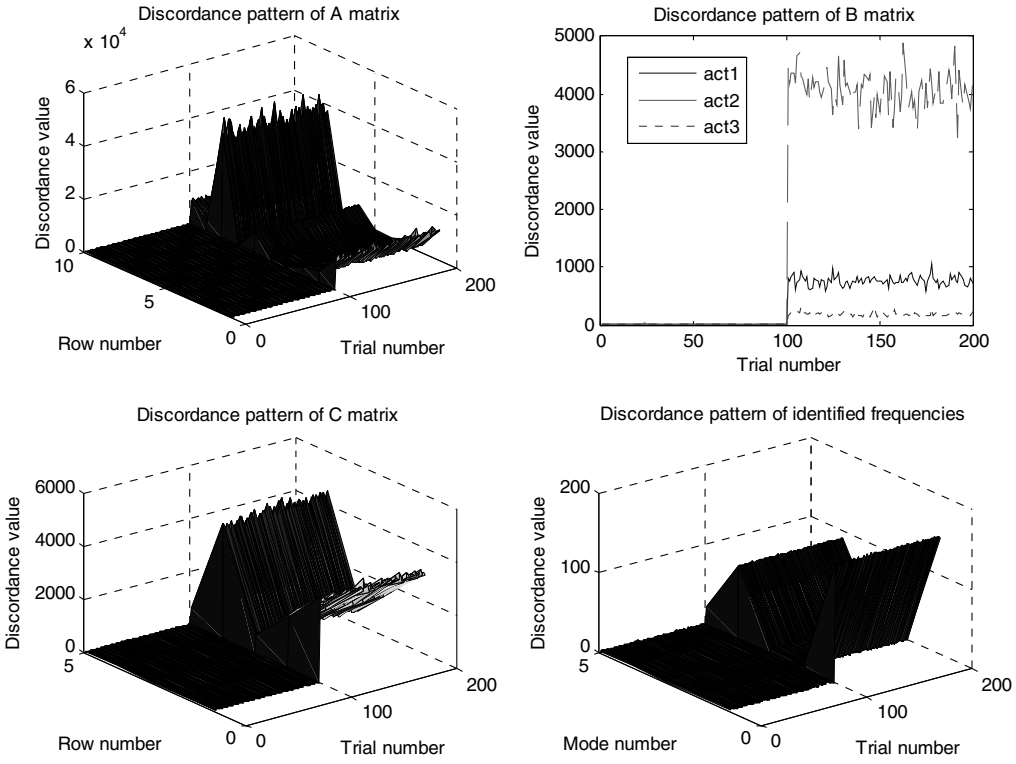

Fig. 4 Discordance pattern of a structure-damage system.

or damaged actuator, the A, B, and C matrices show a large discordance change, whereas the identified frequencies do not. These unique phenomena can be used to classify different damage types.

In multi-actuator systems, when one of the actuators fails, the output of the system will be different from that of the healthy system, but the output time histories will still contain the spectral properties of the system as long as the other actuators are still functioning. This is in comparison with the output of a single-actuator system, in which the system response will decay to zero when the only actuator totally fails. This difference leads to some different phenomena in the outlier analysis. Similarly, the five different types of system failures have also been studied for the single-input system, which lead to slightly different outlier patterns when compared with the same kind of failure in a multi-input system [37].

To develop an automated failure-detection-and-classification algorithm using the unique phenomena associated with different damage types requires the selection of proper features to successfully describe the discordance patterns. By analyzing the phenomenon

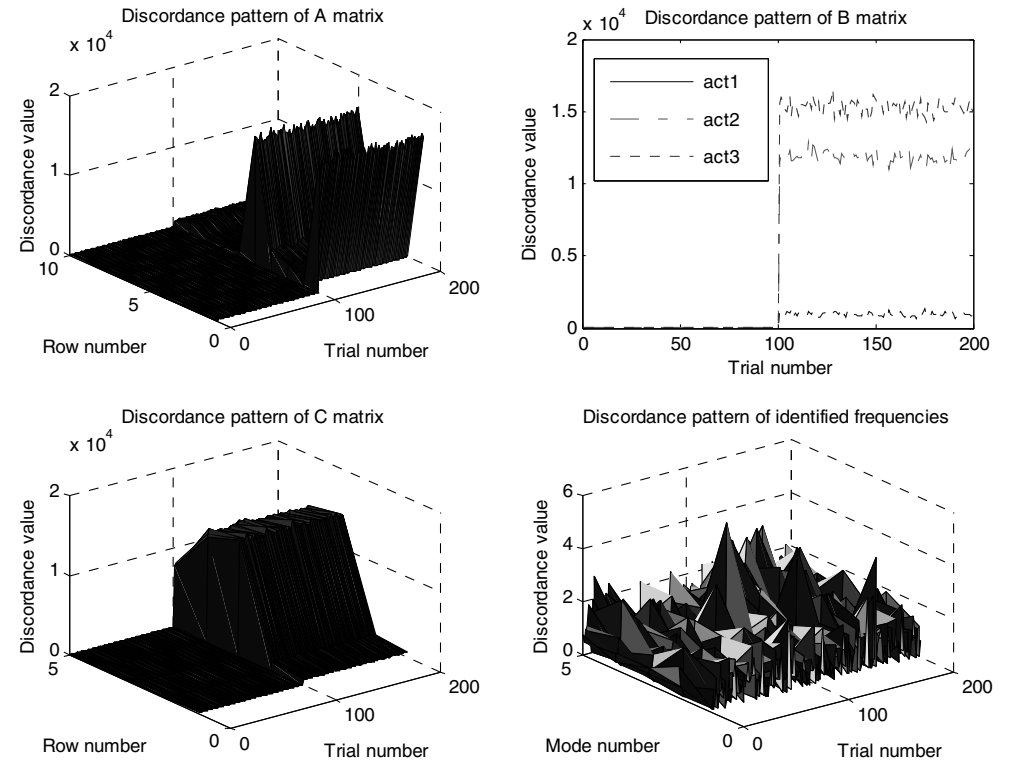

Fig. 5 Discordance pattern of an actuator-damage system.

Table 1 Coefficients used for failure detection and classification

Coefficient	Symbol
Average discordance change of A	$A_{\text{dis}_{\text{chg}}}$
Average discordance change of B	$B_{\text{dis}_{\text{chg}}}$
Average discordance change of C	$C_{\text{dis}_{\text{chg}}}$
Peak ratio of the row discordance of C	$C_{\text{disrow}_{\text{peak}}}$
Average discordance change of frequencies	f_{chg}
Average norm of C matrices (current system)	n_{cc}

related to different damages, six coefficients (shown in Table 1) are used to quantify the change of system parameters.

Coefficients $A_{\text{dis}_{\text{chg}}}$, $B_{\text{dis}_{\text{chg}}}$, and $C_{\text{dis}_{\text{chg}}}$ represent the discordance change level of system parameters. The definitions are given as

$$A_{\text{dissum}}(k) = \sum_{i=1}^{n} A_{\text{dis}}(i,k), \qquad A_{\text{dis}_{\text{chg}}} = \frac{\sum_{k=101}^{200} A_{\text{dissum}}(k)}{\sum_{k=1}^{100} A_{\text{dissum}}(k)} \tag{5}$$

$$B_{\text{dissum}}(k) = \sum_{i=1}^{r} B_{\text{dis}}(i,k), \qquad B_{\text{dis}_{\text{chg}}} = \frac{\sum_{k=101}^{200} B_{\text{dissum}}(k)}{\sum_{k=1}^{100} B_{\text{dissum}}(k)} \tag{6}$$

$$C_{\text{dissum}}(k) = \sum_{i=1}^{m} C_{\text{dis}}(i,k), \qquad C_{\text{dis}_{\text{chg}}} = \frac{\sum_{k=101}^{200} C_{\text{dissum}}(k)}{\sum_{k=1}^{100} C_{\text{dissum}}(k)} \tag{7}$$

where A_{dis}, B_{dis}, and C_{dis} are the discordances of each observation, computed using the Mahalanobis distance defined by Eq. (3). Note that each row of the A and C matrices and each column of the B matrices are considered observations. The variables n, r, and m are the number of states, inputs, and sensors, respectively. As shown in Eq. (5), the sum of the discordances of the state matrix A in each realization A_{dissum} is first computed. Dividing the sum of the A_{dissum} of the current system by that of the healthy system, the outlier level of the A matrices is obtained. The same process is used for the B and C matrices. Recall that realizations 1–100 correspond to the healthy system and the realizations 101–200 correspond to the current system.

Another coefficient ($C_{\text{disrow}_{\text{peak}}}$, the peak ratio of matrix C) is introduced to evaluate the difference of the outliers for different rows of the C matrix and is defined as

$$C_{\text{disrow}(i)} = \text{mean}[C_{\text{dis}}(i, 101{:}200)] \qquad (i = 1, \ldots, m) \tag{8}$$

$$C_{\text{disrow}_{\text{sort}}} = \text{sort}(C_{\text{disrow}}) \tag{9}$$

$$C_{\text{disrow}_{\text{peak}}} = \frac{C_{\text{disrow}_{\text{sort}}}(m)}{C_{\text{disrow}_{\text{sort}}}(m-1)} \tag{10}$$

where the sort operator of Eq. (9) takes the elements in the vector C_{disrow} and sorts them in ascending order.

Similarly, another coefficient f_{chg} can be obtained by dividing the discordance summation of identified frequencies of the current system by that of the healthy system. It quantifies the level of change in the damped natural frequencies of the current system:

$$f_{\text{chg}} = \frac{\sum_{i=1}^{n/2} \sum_{k=101}^{200} f_{\text{dis}}(i,k)}{\sum_{i=1}^{n/2} \sum_{k=1}^{100} f_{\text{dis}}(i,k)} \tag{11}$$

where n is the number of states and $n/2$ is the number of system dynamic modes.

According to the different discordance patterns of different damages, we expect that different failure states would result in large differences in these coefficients. Several simulations of different damage scenarios were performed using the same underlying model. Representative values of these coefficients are shown in Table 2 for different types of damage. Note that for the healthy system, the values of $A_{\text{dis}_{\text{chg}}}$, $B_{\text{dis}_{\text{chg}}}$, and $C_{\text{dis}_{\text{chg}}}$ are all relatively small (shown in bold in Table 2), but when there is any form of damage, one or more of these coefficients become quite large; this fact can be used to determine the existence of a failure.

For a multi-input system,

1) When a sensor is either dead or damaged, we note that $C_{\text{disrow}_{\text{peak}}}$ becomes quite large.

2) When structural damage happens, coefficient f_{chg} gets large.

The preceding observations also hold for a single-input system. In addition, the single-input system exhibits some unique characteristics. When the only actuator is dead, the data analyzed are just noise. In this case, there is a large change in the identified natural frequencies f_{chg} and the value of n_{cc} becomes very small. These observations of the multi-input and single-input systems are used to develop the diagnosis process.

IV. Expert System and Experimental Validation

A diagnosis process is developed based on the simulation results. This process entails monitoring the changes of the coefficients defined by Eqs. (5–11) and comparing them to the generalized upper limits based on data taken from the baseline, or healthy, system. Based on the predefined adaptive diagnosis rules, system failure can be detected and the type of the failure can be classified.

Figure 6 shows the general logic of the diagnosis process. The discordances of the A, B, and C matrices and identified frequencies, as well as the norm of the C matrix, are used as the inputs to the expert system. When one or more of the A, B, or C state-space matrices have a large discordance, the system will be classified as having some form of failure, then the discordance of the C matrix is examined first. If one row shows extreme peak discordance and the discordance of the identified frequencies is small, the system will be classified as having a sensor failure and the sensor corresponding to the row number is identified as the failed sensor.

If a sensor failure is not detected, the discordance of the identified frequencies will be used to determine if actuator damage exists in the system. The system is classified as actuator failure if the identified frequencies do not show large outliers. Note that the actuator damage here can be an amplification change, extreme noise level, or one of

Table 2 Outlier levels corresponding to different damages

		$A_{\text{dis}_{\text{chg}}}$	$B_{\text{dis}_{\text{chg}}}$	$C_{\text{dis}_{\text{chg}}}$	n_{cc}	$C_{\text{disrow}_{\text{peak}}}$	f_{chg}
Healthy system		**1.09e + 0**	**1.23e + 0**	**1.17e + 0**	1.18e + 1	1.00e + 0	1.07e + 0
Multi-input System	Sensor damaged	1.94e + 0	1.14e + 0	5.82e + 1	1.13e + 1	**1.11e + 2**	1.14e + 0
	Sensor dead	2.39e + 2	1.02e + 1	3.79e + 3	1.10e + 1	**4.18e + 1**	2.60e + 0
	Structural damaged	2.56e + 3	1.30e + 2	2.31e + 2	1.38e + 1	1.38e + 0	**7.83e + 1**
	Actuator dead	3.45e + 7	2.24e + 7	2.20e + 3	5.09e + 0	2.31e + 0	2.45e + 0
	Actuator damaged	1.13e + 1	2.07e + 3	1.57e + 1	1.16e + 1	4.14e + 0	1.84e + 0
Single-input system	Sensor damaged	3.25e + 1	1.33e + 0	1.43e + 2	1.16e + 1	**1.00e + 2**	1.50e + 0
	Sensor dead	5.50e + 0	1.18e + 0	4.28e + 3	1.22e + 1	**2.74e + 2**	3.45e + 0
	Structural damaged	1.52e + 3	1.48e + 1	2.25e + 3	1.81e + 1	2.58e + 0	**9.19e + 1**
	Actuator dead	1.18e + 2	6.71e + 0	4.18e + 3	**4.31e−3**	1.52e + 0	**5.29e + 1**
	Actuator damaged	2.29e − 1	1.49e + 0	3.41e + 3	2.40e + 1	2.93e + 0	1.47e + 0

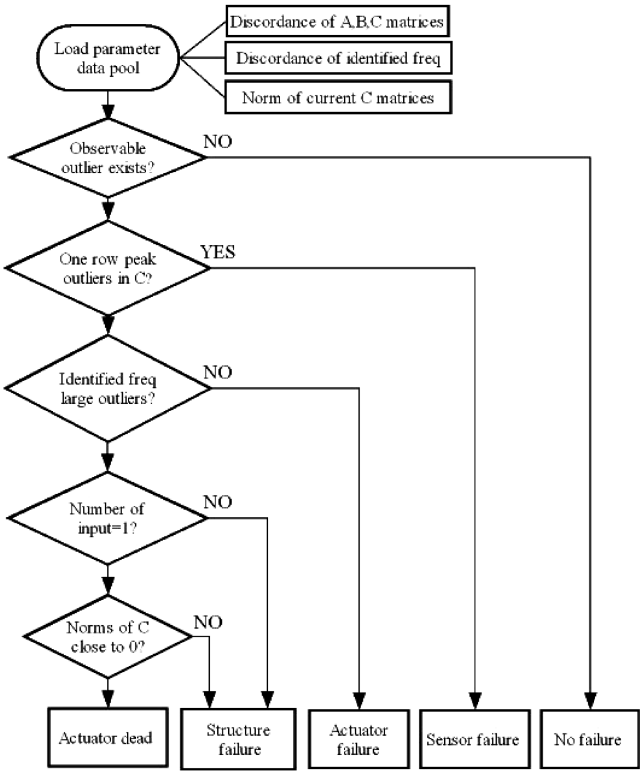

Fig. 6 Diagnosis process for failure detection and classification.

the actuators completely dead in a multi-input system. Complete actuator death of a single-input system is not included here.

For multi-input systems, after excluding sensor failure and actuator failure, the diagnosis process classifies the system damage as structural damage directly. But for a single-input system, the complete death of the only actuator and a structural failure both lead to the large change of the identified natural frequencies. If the norm of the output influence matrix C is very small and close to zero, we classify the single-input system as "actuator dead"; if not, it is classified as a structural failure.

The thresholds for the discordance coefficients are generalized from simulation results and are listed in Table 3. They are incorporated with the idea of the diagnosis process, and an expert system is developed. Simulations show that the expert system works successfully in detecting and classifying different system failures.

Data from an experimental setup, as shown in Fig. 7, are used for the validation of the diagnosis process. The experimental setup is a welded rectangular steel frame with bolted cross members [38]. Data include the acceleration time histories of 32 sensors and the measured impulse response of both the healthy system and structurally damaged system.

The diagonal cross members were bolted to the triangular plates welded into the corners formed by the vertical and horizontal members. The nominal bolt torque was 48 in. $\cdot$ lb. After recording the impulse response of the healthy system, the torque on one of the bolts was reduced to 30 in. $\cdot$ lb to simulate a damaged system. The stiffness of the structure is changed so that it can be viewed as a structural damage. The discordance change of system parameters are

Table 3 Benchmarks for failure identification and classification

Coefficients	Benchmarks	Used for classifying
$A_{\mathrm{dis}_{\mathrm{chg}}}$	>10	System failure
$B_{\mathrm{dis}_{\mathrm{chg}}}$	>10	System failure
$C_{\mathrm{dis}_{\mathrm{chg}}}$	>10	System failure
$C_{\mathrm{disrow}_{\mathrm{peak}}}$	>10	Sensor failure
f_{chg}	>10	Actuator failure
n_{cc}	$<1\mathrm{e}-2$	Total actuator failure in single-input system

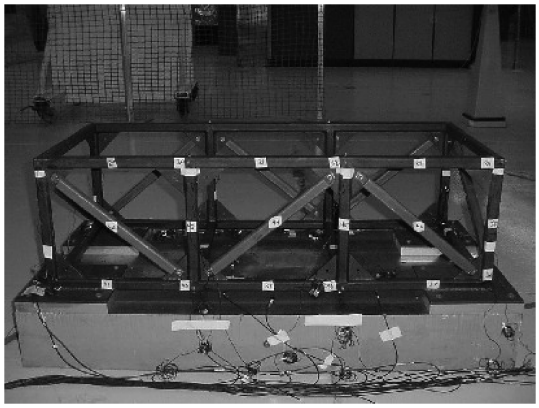

Fig. 7 Configuration of the three-dimensional steel frame.

calculated and are shown in Fig. 8. In this example, the first 50 realizations correspond to the healthy system and the second 50 correspond to the damaged system.

The values of the classification coefficients are shown in the first row of Table 4. The coefficients $A_{\mathrm{dis}_{\mathrm{chg}}}$, $B_{\mathrm{dis}_{\mathrm{chg}}}$, and $C_{\mathrm{dis}_{\mathrm{chg}}}$ are all larger than 10, and so there is some form of failure. Because $C_{\mathrm{disrow}_{\mathrm{peak}}}$ is smaller than 10, a sensor failure is excluded. Because f_{chg} is greater than 10, there is only one input, and n_{cc} is far larger than $1\mathrm{e}-2$, the diagnosis process successfully concludes a structural failure.

Next, using the impulse response data of the healthy system, the healthy output of the 20th sensor is multiplied by a coefficient of 0.6 to simulate sensor damage. The discordance patterns and values of decision coefficients are shown in Fig. 9 and Table 4. The large value of the first three coefficients indicates that there is failure in the system. The peak ratio of C ($C_{\mathrm{disrow}_{\mathrm{peak}}}$) is $4.43\mathrm{e}+3$ (larger than 10), and so a sensor failure is correctly detected. The diagnosis process also shows that the peak happens in the 20th row of the output influence matrix, and so the origin of the failure is also isolated.

Another group of experimental data are used for the validation of an actual actuator failure [39]. The test bed is a 4.0-m-long truss structure with two electromagnetic shakers serving as independent actuators. One of the command inputs of the system is replaced by zero in the time interval of 10–12.5 s. The command input and actual output in this time interval are used for realizations of the current system. According to the diagnosis coefficients shown in Table 4, the large value of the first three coefficients indicates that there is failure in the system. Both values of $C_{\mathrm{disrow}_{\mathrm{peak}}}$ and f_{chg} are less than 10, and so sensor failure and structural damage are excluded. So the expert system successfully detects a failure and classifies its origin to be one of the actuators.

V. Conclusions

This work uses the eigensystem realization algorithm and outlier analysis to build a new methodology for failure detection and classification. According to the different outlier patterns of the system parameters for different failure types, six coefficients were chosen to quantitatively isolate the failure as either a structural, actuator, or sensor failure. A diagnosis process was developed by comparing the values of the coefficient to thresholds obtained from simulations. In the case of a sensor failure, the location of the failed sensor can even be isolated by this technique. Compared with most of

Table 4 Decision coefficients of actual damaged systems

$A_{\mathrm{dis}_{\mathrm{chg}}}$	$B_{\mathrm{dis}_{\mathrm{chg}}}$	$C_{\mathrm{dis}_{\mathrm{chg}}}$	n_{cc}	$C_{\mathrm{disrow}_{\mathrm{peak}}}$	f_{chg}
		Structurally damaged			
$1.54\mathrm{e}+12$	$4.70\mathrm{e}+5$	$5.19\mathrm{e}+6$	$3.14\mathrm{e}+4$	$2.52\mathrm{e}+0$	$3.89\mathrm{e}+3$
		Sensor damaged			
$1.98\mathrm{e}+0$	$1.93\mathrm{e}+0$	$3.28\mathrm{e}+4$	$2.82\mathrm{e}+4$	$4.43\mathrm{e}+3$	$2.20\mathrm{e}+0$
		Actuator damaged			
$1.73\mathrm{e}+6$	$2.87\mathrm{e}+6$	$1.63\mathrm{e}+3$	$1.39\mathrm{e}+1$	$1.39\mathrm{e}+0$	$1.44\mathrm{e}+0$

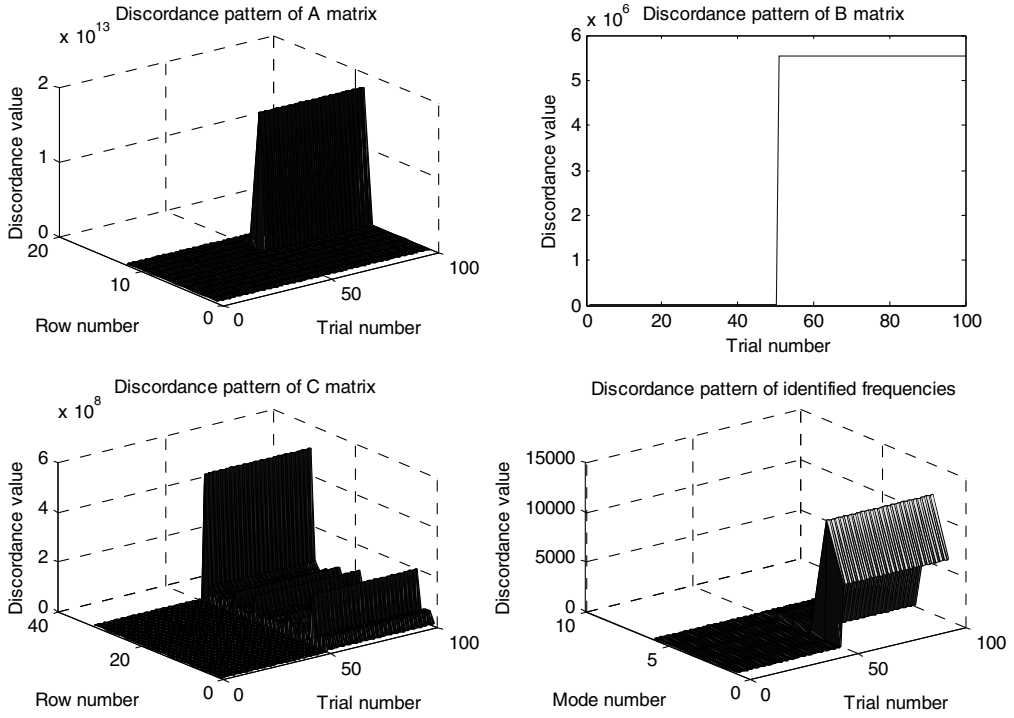

Fig. 8 Discordance pattern of an actual structure-damage system.

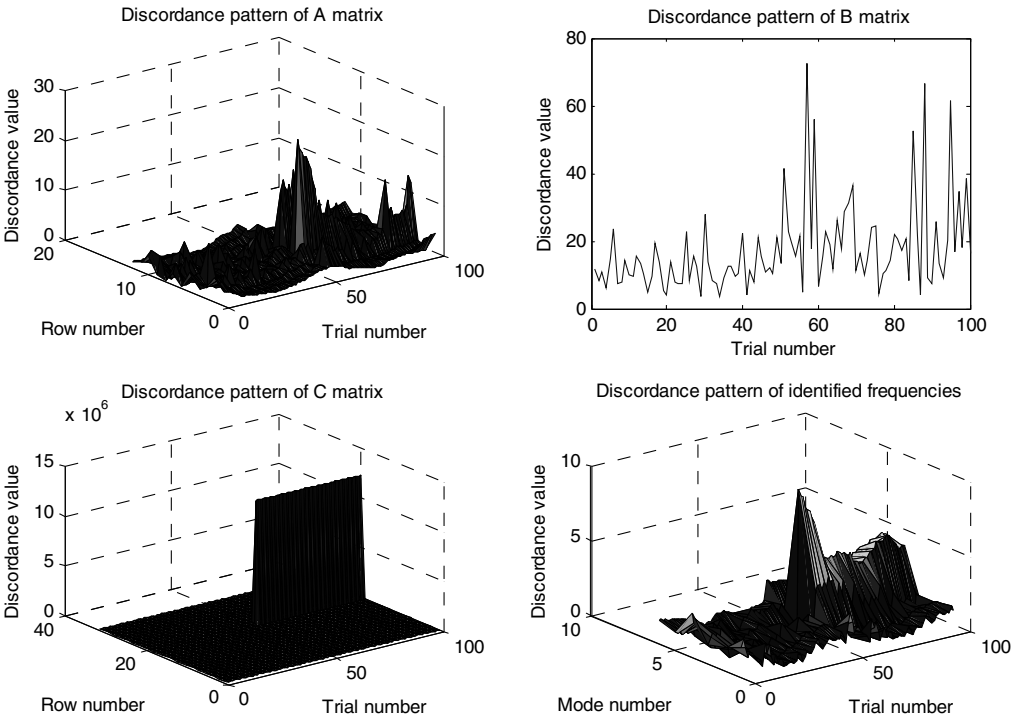

Fig. 9 Discordance pattern of an actual sensor-damage system.

the previous research, which only concerns either structural integrity or sensor FDI independently, this work brings the total, global health-monitoring approach to a more practical and general field. Both simulated numerical examples and experimental data prove the efficiency and accuracy of this failure-detection-and-classification process.

Acknowledgment

The authors wish to acknowledge the support of the Texas Institute for Intelligent Bio-Nano Materials and Structures for Aerospace Vehicles, funded by NASA cooperative agreement no. NCC-1-02038. Any opinions, findings, conclusions, or recommendations expressed in this material are those of the authors and do not necessarily reflect the views of NASA.

References

[1] Isermann, R., "Process Fault Detection Based on Modeling and Estimation Methods: A Survey," *Automatica*, Vol. 20, No. 4, 1984, pp. 387–404.

[2] Willsky, A. S., "A Survey of Design Methods for Failure Detection in Dynamic Systems," *Automatica*, Vol. 12, No. 6, 1976, pp. 601–611.

[3] Basseville, M., "Detecting Changes in Signals and Systems: A Survey,"

Automatica, Vol. 24, No. 3, 1988, pp. 309–326.

[4] Patton, R. J., "Fault Tolerant Control: The 1997 Situation," *Proceedings of the IFAC Symposium: SAFEPROCESS'97*, Vol. 2, International Federation of Automatic Control, Oxford, England, U.K., 1997.

[5] Patton, R. J., "Robustness in Model-Based Fault Diagnosis: The 1995 Situation," *IFAC Workshop: On-Line Fault Detection and Supervision in the Chemical Process Industries*, International Federation of Automatic Control, Oxford, England, U.K., 1995.

[6] Frank, P. M., "Fault Diagnosis in Dynamic Systems Using Analytical and Knowledge-Based Redundancy: A Survey and Some New Results," *Automatica*, Vol. 26, No. 3, 1990, pp. 459–474.

[7] Gertler, J. J., "Survey of Model-Based Failure Detection and Isolation in Complex Plants," *IEEE Control Systems Magazine*, Vol. 8, No. 6, 1995, pp. 3–11.

[8] Isermann, R., "Model Based Fault Detection and Diagnosis Methods," *Proceedings of the 1995 American Control Conference*, American Automatic Control Council, Evanston, IL, 1995, pp. 1605–1609.

[9] Doebling, S. W., Farrar, C. R., Prime, M. B., and Shevitz, D. W., "Damage Identification and Health Monitoring of Structural and Mechanical Systems from Changes in Their Vibration Characteristics: A Literature Review," Los Alamos National Lab., Rept. LA-13070-MS, Los Alamos, NM, 1996.

[10] Doebling, S. W., Farrar, C. R., Prime, M. B., and Shevitz, D. W., "A Review of Damage Identification Methods That Examine Changes in Dynamic Properties," *Shock and Vibration Digest*, Vol. 30, No. 2, 1998, pp. 91–105.

[11] Sohn, H., Farrar, C. R., Hemez, F. M., Shunk, D. D., Stinemates, D. W., and Nadler, B. R., "A Review of Structural Health Monitoring Literature: 1996–2001," Los Alamos National Lab., Rept. LA-13976-MS, Los Alamos, NM, 2003.

[12] Abdalla, M. O., Grigoriadis, K. M., and Zimmerman, D. C., "Enhanced Structural Damage Detection Using Alternating Projection Methods," *AIAA Journal*, Vol. 36, No. 7, 1998, pp. 1305–1311.

[13] Pappa, R. P., James, G. H., and Zimmerman, D. C., "Autonomous Modal Identification of the Space Shuttle Tail Rudder," *Journal of Spacecraft and Rockets*, Vol. 35, No. 2, 1998, pp. 163–169.

[14] Zimmerman, D. C., Yap, K., and Hasselman, T., "Evolutionary Approach for Model Refinement," *Mechanical Systems and Signal Processing*, Vol. 13, July 1999, pp. 609–625.

[15] Kaouk, M., and Zimmerman, D. C., "Structural Damage Assessment Using a Generalized Minimum Rank Perturbation Theory," *AIAA Journal*, Vol. 32, No. 4, 1992, pp. 836–842.

[16] Zimmerman, D. C., "Looking into the Crystal Ball: The Continued Need for Multiple Viewpoints in Damage Detection," *Key Engineering Materials*, Vol. 167–168, June 1999, pp. 76–90.

[17] Atalla, M. J., and Inman, D. J., "On Model Updating Using Neural Networks," *Mechanical Systems and Signal Processing*, Vol. 12, No. 1, 1998, pp. 135–161.

[18] Zang, C., and Imregun, M., "Structural Damage Detection Using Artificial Neural Networks and Measured FRF Data Reduced Via Principal Component Projection," *Journal of Sound and Vibration*, Vol. 242, May 2001, pp. 813–827.

[19] Wang, W. J., Wu, Z. T., and Chen, J., "Fault Identification in Rotating Machinery Using the Correlation Dimension and Bispectra," *Nonlinear Dynamics*, Vol. 25, No. 4, Aug. 2001, pp. 383–393.

[20] Ibrahim, S. R., and Mikulcik, E. C., "A Method for the Direct Identification of Vibration Parameters from the Free Response," *Shock and Vibration Bulletin*, Vol. 47, No. 4, 1977, pp. 183–198.

[21] Ibrahim, S. R., and Pappa, R. S., "Large Model Survey Testing Using the Ibrahim Time Domain Identification Technique," *Journal of Spacecraft and Rockets*, Vol. 19, No. 5, 1982, pp. 459–465.

[22] Vold, H., Kundrat, J., Rocklin, G. T., and Russell, R., "A Multiple-Input Modal Estimation Algorithm for Mini Computers," *SAE Transactions*, Vol. 91, No. 1, 1982, pp. 815–821.

[23] Juang, J. N., and Pappa, R. S., "An Eigensystem Realization Algorithm for Model Parameter Identification and Model Reduction," *Journal of Guidance, Control, and Dynamics*, Vol. 8, No. 5, 1985, pp. 620–627.

[24] Zimmerman, D. C., and Lyde, T. L., "Sensor Failure Detection and Isolation in Flexible Structures Using the Eigensystem Realization Algorithm," *Journal of Guidance, Control, and Dynamics*, Vol. 16, No. 3, 1993, pp. 490–497.

[25] Juang, J. N., Phan, M., Horta, L. G., and Longman, R. W., "Identification of Observer/Kalman Filter Markov Parameters: Theory and Experiments," *Journal of Guidance, Control, and Dynamics*, Vol. 16, No. 2, 1993, pp. 320–329.

[26] Phan, M., Horta, L. G., Juang, J. N., and Longman, R. W., "Improvement of Observer/Kalman Filter Identification (OKID) by Residual Whitening," *Journal of Vibration and Acoustics*, Vol. 117, No. 2, 1995, pp. 232–239.

[27] Dyke, S. J., Caicedo, J. M., and Johnson, E. A., "Monitoring of a Benchmark Structure for Damage Identification," *Proceedings of the 14th ASCE Engineering Mechanics Conference* [CD-ROM], American Society of Civil Engineers, Reston, VA, 2000.

[28] Caicedo, J. M., Dyke, S. J., and Johnson, E. A., "Health Monitoring Based on Component Transfer Functions," *Advances in Structural Dynamics*, edited by J. M. Ko and Y. L. Xu, Vol. 2, Elsevier, New York, 2000, pp. 997–1004.

[29] Lus, H., and Betti, R., "Damage Identification in Linear Structural Systems," *Proceedings of the 14th ASCE Engineering Mechanics Conference* [CD-ROM], American Society of Civil Engineers, Reston, VA, 2000.

[30] Bernal, D., and Gunes, B., "Observer/Kalman and Subspace Identification of the UBC Benchmark Structural Model," *Proceedings of the 14th ASCE Engineering Mechanics Conference* [CD-ROM], American Society of Civil Engineers, Reston, VA, 2000.

[31] Zimmerman, D. C., and Lyde, T. L., "Sensor Failure Detection and Isolation in Flexible Structures Using the Eigensystem Realization Algorithm," *Journal of Guidance, Control, and Dynamics*, Vol. 16, No. 3, 1993, pp. 490–497.

[32] Juang, J., "System Realization Theory," *Applied System Identification*, Prentice–Hall, Upper Saddle River, NJ, 1994, pp. 121–170.

[33] Kailath, K., "State-Space and Matrix-Fraction Description," *Linear Systems*, Prentice–Hall, Upper Saddle River, NJ, 1980, pp. 364–365.

[34] Worden, K., Manson, G., and Fieller, N. J., "Damage Detection Using Outlier Analysis," *Journal of Sound and Vibration*, Vol. 229, No. 3, 2000, pp. 647–667.

[35] Sohn, H., Farrar, C. R., Hunter, N. F., Wirdeb, K., "Structural Health Monitoring Using Statistical Pattern Recognition Techniques," *Journal of Dynamic Systems, Measurement, and Control*, Vol. 123, No. 4, 2001, pp. 706–711.

[36] Barnett, V., and Lewis, T., "Univariate Data," *Outliers in Statistical Data*, 3rd ed., Wiley, New York, 1994, pp. 143–189.

[37] Shen, S., "Damage Detection and Classification Using ERA and Outlier Analysis," M.S. Thesis, Univ. of Houston, Houston, TX, Aug. 2005.

[38] Taylor, S., and Zimmerman, D. C., "Damage Detection in a Cargo Bay Frame Using Ritz Vectors," *Proceedings of SEM IMAC 23* [CD-ROM], Society for Experimental Mechanics, Bethel, CT, 2005.

[39] Koh, B. H., Li, Z., Dharap, P., and Nagarajaiah, S., "Actuator Failure Detection Through Interaction Matrix Formulation," *Journal of Guidance, Control, and Dynamics*, Vol. 28, No. 2, 2005.